

NASA TECHNICAL NOTE



NASA TN D-3140

2.1

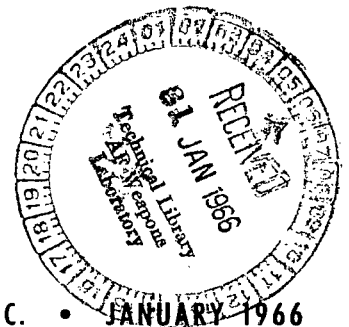
NASA TN D-3140



FOR IN COPY: RETURN
APRIL (WILLIS)
KURTLAND J. ...

A STUDY OF THE ACCURACY OF ESTIMATING THE ORBITAL ELEMENTS OF A LUNAR SATELLITE BY USING RANGE AND RANGE-RATE MEASUREMENTS

*by Harold R. Compton
Langley Research Center
Langley Station, Hampton, Va.*



TECH LIBRARY KAFB, NM



0130136

NASA TN D-3140

A STUDY OF THE ACCURACY OF ESTIMATING THE ORBITAL
ELEMENTS OF A LUNAR SATELLITE BY USING RANGE
AND RANGE-RATE MEASUREMENTS

By Harold R. Compton

Langley Research Center
Langley Station, Hampton, Va.

NATIONAL AERONAUTICS AND SPACE ADMINISTRATION

For sale by the Clearinghouse for Federal Scientific and Technical Information
Springfield, Virginia 22151 - Price \$2.00

A STUDY OF THE ACCURACY OF ESTIMATING THE ORBITAL
ELEMENTS OF A LUNAR SATELLITE BY USING RANGE
AND RANGE-RATE MEASUREMENTS

By Harold R. Compton
Langley Research Center

SUMMARY

A parametric study has been made to determine the effects of tracking mode and orbital parameters on the accuracy of determining the state of a lunar satellite. A comparison of the relative advantage of using either range or range-rate measurements was made, and the results indicate that the advantage of one data type over the other is very dependent on the semimajor axis and somewhat dependent on the nodal position and eccentricity but is not dependent on the inclination. For example, it was found that for lunar orbits with medium eccentricity and with semimajor axes of approximately 2500 kilometers, the orbital elements could be determined with equal accuracy by using either range or range-rate data when the ratio of the standard deviation of range measurements to the standard deviation of range-rate measurements was approximately 1500 seconds. For lunar orbits with semimajor axes smaller than approximately 2500 kilometers, range-rate measurements gave a more accurate determination of the elements, whereas for orbits with semimajor axes greater than approximately 2500 kilometers, range measurements proved to be the better data type of the two. It was also found that range and range-rate measurements are similar data types in that they produce similar correlation matrices for the state variables and simultaneous use of both data types does not significantly reduce correlations between the elements.

Over a range of inclination angles from 2° to 40° with respect to the earth-moon plane, the results showed that the accuracy of determining the orientation angles increased as the inclination increased whereas the accuracy of determining the in-plane variables remained nearly constant. The effects of variations in the nodal position on the accuracy of determining the orbital elements were found to be periodic. The eccentricity, argument of periapsis, and the longitude of the ascending node were best determined when the orbit was viewed on edge whereas the semimajor axis, inclination, and the time of periapsis passage were best determined when the orbit was viewed broadside. It was also found that the accuracy of estimating the elements increased with an increase in eccentricity.

INTRODUCTION

Current plans for lunar research missions include the establishment of satellites in orbit about the moon. For unmanned missions the elements of the orbit in which the vehicle is moving must be known within a reasonable degree of accuracy in order to determine the location of the satellite when data are taken by the satellite. For manned missions the position must be known with a high degree of accuracy. The knowledge of the orbital elements may also be used to determine certain selenodetic constants and in particular the coefficients of the harmonics of the lunar gravitational field. It is therefore of interest to investigate the accuracy to which the orbital elements of a lunar satellite can be determined by earth-based tracking.

The basic earth-based data types are range, range-rate, and angular measurements. Since the accuracy of making angular measurements of a vehicle moving in orbit about the moon is low, this particular data type was not considered. Hence the results presented in this paper are based solely on the use of range and range-rate measurements. It is of interest not only to estimate the accuracy to which the elements can be determined but also to ascertain the relative advantage of one data type over the other. Therefore a parametric study in which both data types were used was initiated.

In order to make the parametric study, the statistical equations which were used to estimate the accuracy to which the orbital elements could be determined were programed in double precision on an IBM 7094 electronic data processing system. The basic theory and equations used in the program are given in appendixes A and B.

SYMBOLS

Unless otherwise specified, the unit of length is the lunar radius, which is 1738 kilometers, and the unit of time is the period of a lunar surface satellite divided by 2π , which is 1035 seconds. The coordinate system and angular parameters are illustrated in figure 1.

A,B	matrices containing partial derivatives of a given data type with respect to orbital elements
a	semimajor axis of lunar satellite orbit
E	eccentric anomaly; operator used in appendix A
e	eccentricity of lunar satellite orbit
f_i	functional relation between observable quantity and parameters to be estimated (see eq. (A2))
i	inclination of orbital plane of lunar satellite to earth-moon plane

l_{1,m_1,n_1}	} direction cosines (see appendix B)
l_{2,m_2,n_2}	
M	mean anomaly
N	number of observations
n	mean angular rate of lunar satellite
P	position of lunar satellite
Q	weighted least squares function defined in equation (A7)
R	distance from center of earth to center of moon
r	distance from center of moon to lunar satellite
\bar{r}	vector from center of moon to lunar satellite
t	time
t_i	time of i th measurement
t_0	time of periapsis passage
v	true anomaly
W	weighting matrix
X,Y,Z	coordinate axes with origin at center of moon (The X-axis is positive in the direction from the center of the moon away from the center of the earth, the Y-axis is positive in the direction of rotation of the moon, and the Z-axis is positive in such a direction that it forms a right-handed axis system.)
x,y,z	position components of lunar satellite
y_i	i th measurement of general quantity y , where $i = 1, 2, \dots, N$
α	parameter to be estimated (subscript denotes particular parameter)
ϵ	error
ϵ_i	error in i th measurement
$\theta = \omega + v$	

Λ_{α}	covariance matrix of estimated parameters
μ	gravitational constant of moon
ξ	mean motion of moon about earth
ρ	range or distance from center of earth to position of lunar satellite; in appendix A the symbol ρ is used with double subscripts to denote the correlation between the variables indicated by the subscripts
ρ_i	i th measurement of ρ
$\bar{\rho}$	vector from center of earth to position of lunar satellite
$\dot{\rho}$	range rate or radial velocity of lunar satellite with respect to center of earth
$\dot{\rho}_i$	i th measurement of $\dot{\rho}$
σ	standard deviation or one-sigma uncertainty (When this symbol appears with a subscript, it is taken to mean the one-sigma uncertainty in the estimation of the variable indicated by the subscript.)
ω	argument of periapsis, angle measured in lunar satellite plane from ascending node to periapsis
Ω	longitude of ascending node of lunar satellite orbital plane measured in earth-moon plane in direction of rotation of moon from positive X-axis
Ω'	longitude of ascending node measured in YZ-plane (see sketch 1)

ANALYSIS

In order to simplify the problems associated with the analysis in this study, certain assumptions were made. The moon was assumed to be a point mass rotating about the earth in a circular orbit. A single observation station making uncorrelated, unbiased range and range-rate measurements of a lunar satellite moving in a two-body orbit and not occulted by the moon was assumed to be located at the center of the earth. All the results presented were obtained by assuming a constant one-sigma error in the range measurements and range-rate measurements of 15 meters and 0.01 meter per second, respectively. These values are conservative estimates of the tracking data accuracy applicable to the NASA deep space net (DSN) tracking system (see ref. 1). Data were assumed to have been processed for 1, 2, 3, 4, 5, and sometimes 10 consecutive orbits. Usually 26 range and 26 range-rate measurements equally spaced in time were simulated during each orbit.

The fundamental approach made in this error analysis was to simulate range and range-rate measurements over a given period of time and from this simulation to calculate a covariance matrix from which the variances of the elements could be obtained. The covariance matrix was obtained from a weighted least squares simulation. (See appendix A for details of the simulation.) The form of this matrix is

$$\Lambda_{\alpha} = \sigma^2 (A^T A)^{-1} \quad (1)$$

where the (i,j) element of A is equal to the partial derivative of the i th observation with respect to the j th element to be estimated and where σ is the standard deviation of the measurements. Explicit expressions for the partials of range and range rate with respect to the Keplerian elements are given in appendix B. It can be seen from equation (1) that no actual values of the measurements are needed, and in particular only the standard deviation of the observations is used. Therefore, with a fixed tracking schedule and only one type of data, the one-sigma uncertainty in the estimation of the elements is proportional to the standard deviation of the data type. Thus, when the accuracy of estimating the elements is compared for two data types, an important parameter is the ratio of the standard deviations of the data types, for example, $\sigma_{\rho}/\sigma_{\dot{\rho}}$. The covariance matrix for the simultaneous use of two data types is shown in appendix A.

In order to make a parametric study of the effects of a given element on the accuracy of determining the elements, five elements of a chosen nominal orbit were held constant and the sixth was varied over a given range. The one exception to this procedure was in the eccentricity variation for which, instead of the nominal value for the semimajor axis, a value of 5000 kilometers was used. This exception was made in order to insure that over the given range of eccentricities the distance from the center of the moon to the lunar satellite was never less than the radius of the moon. The elements of the nominal orbit used in this investigation were chosen to provide a low periapsis (approximately 50 km) in an orbit with medium eccentricity and inclination. These elements are as follows:

$$a = 2235 \text{ kilometers}$$

$$i = 30^\circ$$

$$\Omega = 30^\circ$$

$$\omega = 180^\circ$$

$$e = 0.2$$

$$t_0 = 0 \text{ second}$$

In this study the angle ω always appears in the partial derivatives as an angle added to the true anomaly v in the argument of either a sine or

cosine function. Inasmuch as the true anomaly rotates through 360° each orbit, the argument of this sine or cosine function rotates through one period regardless of the value of ω . Hence, the effects of a variation in ω upon the accuracy of estimating the elements are negligible as long as integral orbits of tracking are used and occultations are not considered. Similarly, no results are presented for a variation in t_0 , because this parameter only defines where the vehicle is located in the orbit and, as long as measurements are made over complete orbits, the effects of changing t_0 are negligible.

RESULTS AND DISCUSSION

Effects of Tracking Schedule on Accuracy of Estimating the Elements

The partial derivatives contained in the A matrix are fundamental to the entire orbit-determination process. A large derivative is said to have a large information content and, similarly, a small derivative is said to have a small information content. It can be shown that the accuracy of estimating any parameter increases as the information about that parameter increases or hence as the derivative of the observable quantity (range or range rate) with respect to the parameter increases. Figures 2 and 3 are presented to show how the partials of range and range rate with respect to the orbital elements change with time. These derivatives are plotted as functions of time over five orbital periods. The orbital period is approximately 2.6 hours. It can be seen that the partials have a periodic nature with a period equal to that of one orbit.

In figures 2 and 3 the amplitudes of the curves representing the partial derivatives of range and range rate with respect to the semimajor axis continue to increase with time. This increase is due to the mixed secular terms such as $n(t - t_0)\sin E$ which are contained in the analytical expressions for these derivatives. Because the information content of the data increases rapidly with time due to the mixed secular terms, the semimajor axis should be determined more accurately over long time arcs. The amplitudes of the partial derivatives of range and range rate with respect to the inclination appear to be decreasing with time, but the reason for this decrease is the fact that the derivatives vary as $\sin \Omega$ and, in the particular case shown in figures 2 and 3, Ω is 30° at time zero and is decreasing at a rate of 0.54° per hour due to the rotation of the X-axis. Since the amplitude of the partial derivative with respect to inclination is a maximum when $\Omega = 90^\circ$ or $\Omega = 270^\circ$, it is expected that the inclination would be best determined when the orbit is viewed broadside, that is, when Ω equals 90° or 270° . Likewise, a very weak determination of the inclination is expected when $\Omega = 0^\circ$ or $\Omega = 180^\circ$ because, regardless of the inclination, identical time histories of range and range-rate measurements would be obtained - that is, the observations are independent of inclination.

When the orbit is viewed nearly on edge, that is, when Ω is very near 0° or 180° , the partial derivatives of range and range rate with respect to Ω and ω are related through the expressions

$$\frac{\partial \rho}{\partial \Omega} \approx \frac{\partial \rho}{\partial \omega} \cos i \quad (2)$$

$$\frac{\partial \dot{\rho}}{\partial \Omega} \approx \frac{\partial \dot{\rho}}{\partial \omega} \cos i \quad (3)$$

Therefore if the inclination is not large, the derivatives are approximately equal, and figures 2 and 3 show that even with an inclination of 30° and with $\Omega = 30^\circ$ they are not vastly different. If the relations in equations (2) and (3) were always exactly true, the normal matrix $A^T A / \sigma^2$ would be singular and noninvertible, because one column of the A matrix would be proportional to another column and therefore one row of the normal matrix would be proportional to another row. Thus, in a real-orbit-determination process where the measurements are made with the orbit being viewed nearly on edge, the normal matrix is expected to be poorly conditioned for inversion by use of finite-decimal arithmetic.

The special case of near-zero inclination also has problems associated with it. By referring to the equations in appendix B, it can be seen that when i is nearly zero the partial derivatives of range and range rate with respect to Ω and ω are related through the following expressions regardless of the nodal position:

$$\frac{\partial \rho}{\partial \Omega} \approx \frac{\partial \rho}{\partial \omega} \quad (4)$$

$$\frac{\partial \dot{\rho}}{\partial \Omega} \approx \frac{\partial \dot{\rho}}{\partial \omega} \quad (5)$$

Again, the normal matrix is expected to be poorly conditioned for inversion. Thus, trouble might be expected in trying to invert the normal matrix associated with an orbit having near-zero inclination.

No physical significance should be attached to the fact that the partial derivative of range with respect to the eccentricity remains positive as shown in figure 2. This fact is due to the position of the line of nodes during the observation period. The node angle would be different for different observation periods and hence the derivative might be negative.

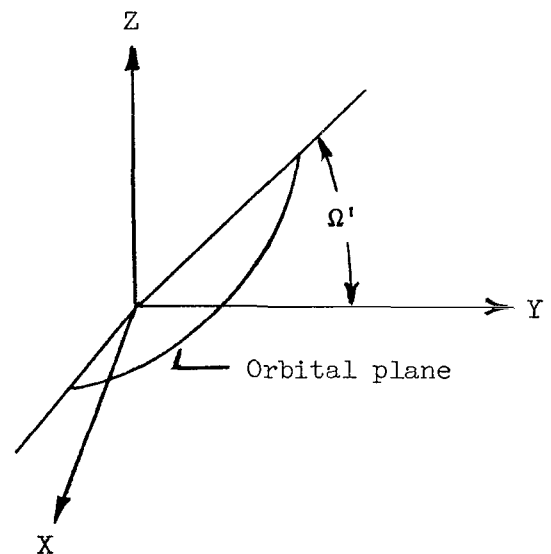
The accuracy of estimating the orbital elements varies significantly with the number of orbits tracked, the number of observations made during each orbit, and the position of the satellite in the orbit at the time of the observations. In order to show how the accuracies vary with the number of orbits tracked, figure 4 is presented. This figure illustrates how well the elements of the nominal orbit could have been determined if the vehicle had been tracked by making range and range-rate measurements every 6 minutes over a period of 1 to 10 orbits. As would be expected, the accuracy of estimating the elements increases with the number of orbits tracked. It is also seen in figure 4 that

range measurements and range-rate measurements having one-sigma errors of 15 meters and 0.01 meter per second, respectively, ($\sigma_\rho/\sigma_{\dot{\rho}} = 1500$ seconds) can be used separately to determine the elements to approximately the same accuracy. It is shown subsequently that this result is due to the particular values of the orbital elements utilized and that in particular the relative advantage of one data type over the other is dependent upon the semimajor axis, the nodal position, and eccentricity. Thus, this result cannot be generalized to include all lunar orbits. The lowest curve in each set of curves presented in figure 4 shows the one-sigma values resulting from the simultaneous use of range and range-rate measurements. These values are, of course, smaller than the values obtained when either data type is used separately.

Interpolation in figure 4 between integral orbits to obtain one-sigma values for fractions of orbits is only approximate, and the reason for this can be understood by referring to the discussion of figures 2 and 3 where it was shown that, in general, the time variation of the partial derivatives is periodic, with a period being equal to that of one orbit. Since the elements of the normal matrix are sums of products of these partial derivatives and since the covariance matrix is the inverse of the normal matrix, it is apparent that the values of the elements of the covariance matrix are largely dependent upon the times at which the observations were made. Therefore if measurements are simulated over a fraction of an orbit, the values of the matrix elements will vary according to the portion of the orbit investigated, and for this reason the curves in figure 4 between integral orbits may not be as smooth as indicated. Hence, interpolation in figure 4 is only approximate.

Before proceeding to other results, it should be noted that in a real orbit determination the covariance matrix associated with tracking the satellite for a single orbital period may be difficult to obtain due to numerical operations in the computer. In particular, the normal matrix may be nearly singular, and experience has shown that single-precision arithmetic is not adequate for inversion of this matrix. During a single orbital period, the moon rotates through a very small angle. Thus, the problem under consideration approaches the stationary-moon problem for which the normal matrix $A^T A / \sigma^2$ becomes singular. The covariance matrix is the inverse of the normal matrix, as was shown in equation (1), and hence it cannot be obtained if the normal matrix is singular.

The following argument shows why the normal matrix is singular when the moon is stationary. It has been shown in reference 2 that, in the case of the stationary moon, range-rate measurements (and it can be similarly shown for range measurements) are independent of the angle Ω' which is defined in sketch 1.



Sketch 1

Therefore, the following relations hold:

$$\frac{\partial \rho}{\partial \Omega'} = 0 \quad (6)$$

$$\frac{\partial \dot{\rho}}{\partial \Omega'} = 0 \quad (7)$$

By writing i , Ω , and ω as functions of Ω' and noting that ρ and $\dot{\rho}$ are functions of i , Ω , and ω , the following equations can be derived from equations (6) and (7) by direct substitution:

$$\cos \Omega \frac{\partial \rho}{\partial i} - \frac{\cos i \sin \Omega}{\sin i} \frac{\partial \rho}{\partial \Omega} + \frac{\sin \Omega}{\sin i} \frac{\partial \rho}{\partial \omega} = 0 \quad (8)$$

$$\cos \Omega \frac{\partial \dot{\rho}}{\partial i} - \frac{\cos i \sin \Omega}{\sin i} \frac{\partial \dot{\rho}}{\partial \Omega} + \frac{\sin \Omega}{\sin i} \frac{\partial \dot{\rho}}{\partial \omega} = 0 \quad (9)$$

The coefficients of the partial derivatives in equations (8) and (9) are the partial derivatives of i , Ω , and ω with respect to Ω' . Equation (8) indicates that $\partial \rho / \partial i$, $\partial \rho / \partial \Omega$, and $\partial \rho / \partial \omega$ are linearly related and hence the A matrix is at most of rank 5. Thus, the normal matrix $A^T A / \sigma^2$ has a rank of at most 5 and is therefore singular and noninvertible. From equation (9) it is clear that the same conclusions hold for range-rate data. Usually if a normal matrix is poorly conditioned for inversion, high correlations between the parameters which cause this poor conditioning can be expected. A high correlation between i , Ω , and ω is therefore expected, and, as shown subsequently, these three parameters are highly correlated.

The problem of determining the elements based on range and range-rate data for a single orbital period is not exactly the stationary-moon problem because the moon has rotated through an angle of 1.5° . However, it is questionable whether 1.5° of rotation is sufficient to reduce the linear relations between i , Ω , and ω enough to allow the normal matrix to become invertible in finite-decimal arithmetic. Experience has shown that single-precision, 8-decimal arithmetic is not adequate to invert the normal matrix associated with one orbit of tracking. This difficulty was circumvented by programing the problem in double precision, that is, 16-decimal arithmetic.

It is of interest to know whether the one-sigma estimation error presented in this report obeys the \sqrt{N} law which states that the one-sigma uncertainty in estimating a parameter is inversely proportional to the \sqrt{N} where N is the number of measurements made. By referring to equation (1), it can be seen that if the partial derivatives which are used in the elements of $A^T A$ were constant, then the one-sigma estimation error would obey the \sqrt{N} law exactly. It has been shown that these derivatives are not constant but periodic and therefore if a sufficient number of measurements were used over the tracking

interval, one would expect the elements of $A^T A$ to be approximately proportional to N . Hence one would expect the one-sigma estimation error to approximately obey the \sqrt{N} law. Figure 5 is presented to show that the data in this report do approximate this law and hence can be generalized to include an arbitrary number of observations. In order to obtain the one-sigma values shown in figure 5, it was assumed that N observations of the satellite were made over five consecutive orbits. This process was repeated several times for the same five orbits but with N changed each time. These one-sigma values were plotted as functions of N on log-log paper in figure 5, and it can be seen that for all six elements the curves have a slope of approximately $-1/2$, as was expected.

In the discussion of figure 4 it was pointed out that the simultaneous use of the two data types produced estimates of the elements which were more accurate than those obtained from the use of either data type alone. However, by referring to figure 5 it can be seen that an accuracy equivalent to that obtained from the simultaneous use of the two data types can be achieved by using more observations of the same data type.

In a real orbit determination, the simultaneous use of several data types would be expected to help eliminate high correlations between the parameters and thereby cause the normal matrix to be better conditioned for inversion. As stated previously, if a normal matrix is poorly conditioned for inversion, high correlations between the parameters causing the poor conditioning can usually be expected. Therefore, it is of interest to know whether the simultaneous use of range and range-rate data serves to eliminate high correlations between the parameters.

The correlation matrices obtained after one orbit by using range, range-rate, and range plus range-rate data are presented in figure 6 (see appendix A for the definition of the correlation matrix). In the previous discussion of the stationary-moon problem, it was pointed out that i , Ω , and ω are expected to be highly correlated after one orbit of tracking, and figure 6 shows that a high correlation does exist. Note that the correlations between these three parameters which were obtained by the simultaneous use of range and range-rate data are not significantly lower than those obtained when either data type is used alone. The correlation matrices after five orbits are shown in figure 7. It can be seen that the parameters i , Ω , and ω are still highly correlated in all three correlation matrices. The correlation between Ω and ω is slightly higher than that between i and Ω and i and ω due to the nearly linear relation between Ω and ω when i is small. A comparison of the three correlation matrices was made after each orbit up to 10 orbits. Except for the one-orbit case, it was found that the three matrices were similar - that is, elements which were highly correlated on one matrix were highly correlated on the other. Hence it was concluded that range and range-rate measurements are similar data types and that their simultaneous use does not produce any appreciable reduction in the correlations.

Effects of Variations in the Elements on the

Accuracy of Determining the State

The effects upon the accuracy of determining the elements due to a variation in the semimajor axis are illustrated in figure 8. This figure is a plot of the one-sigma value of the error in the estimation of the elements after five consecutive orbits of tracking as a function of the semimajor axis. The semimajor axis was varied between 2235 and 5000 kilometers, and i , Ω , ω , e , and t_0 were held constant at the nominal values previously given. For each value of the semimajor axis considered in the present study (2235, 2500, 3500, 4000, 4500, and 5000 km), it was assumed that 26 range and 26 range-rate measurements equally spaced in time were made every orbit for five consecutive orbits. It can be seen that, except for the elements a and t_0 , the accuracy of determining the elements increased as the semimajor axis increased when range measurements alone were used, whereas the accuracy decreased for the elements a , e , and t_0 and increased for the elements i , Ω , and ω when range-rate measurements alone were used. In general, for lunar orbits with semimajor axes of approximately 2500 kilometers, the orbital elements could be determined with equal accuracy by using either range or range-rate data when $\sigma_\rho/\sigma_{\dot{\rho}} \approx 1500$ seconds. For lunar orbits with semimajor axes smaller than approximately 2500 kilometers, range-rate measurements gave a more accurate determination of the elements, whereas for orbits with semimajor axes greater than approximately 2500 kilometers, range measurements proved to be the better data type of the two. Also, it can be noted in figure 8 that the relative advantage of one data type over the other is not constant, that is, the curves diverge. It is concluded that the data type producing the best set of elements is very dependent on the semimajor axis.

A range of satellite orbital inclinations from 2° to 40° with respect to the earth-moon plane was considered. The elements a , Ω , ω , e , and t_0 were held constant at the nominal values while i was varied over the given range. It was assumed that the satellite had been tracked over a period of five consecutive orbits by making 26 range and 26 range-rate observations per orbit equally spaced in time. The results are presented in figure 9. This figure shows typical curves for the variation of the one-sigma error in determining the elements with the sine of the inclination. Over the range of inclinations in the investigation, the accuracy of determining the orientation angles i , Ω , and ω increased significantly as the inclination increased, whereas the accuracy of determining the in-plane elements a , e , and t_0 remained approximately constant. It should be noted that the curves for σ_Ω and σ_ω have a slope of -2 and the curve for σ_i has a slope of -1. Similar plots not presented herein showed that these slopes are independent of the nodal position and hence it was concluded that σ_Ω and σ_ω are inversely proportional to $\sin^2 i$ and that σ_i is inversely proportional to $\sin i$. This result was unexpected inasmuch as it was not apparent from the form of the partial derivatives. It can be seen from figure 9 that over the range of inclinations from 2° to 40° either range or range-rate measurements can be used to determine the elements with approximately equal accuracy when $\sigma_\rho/\sigma_{\dot{\rho}} = 1500$ seconds. It was

concluded from this figure that the relative advantage of one of the data types over the other does not change over the range of inclinations in the present investigation.

The curves shown in figure 10 indicate that the position of the line of nodes during the tracking period is a very significant parameter in the determination of the orbital elements. The results presented in this figure are those obtained by assuming that the satellite had been tracked over a period of five consecutive orbits during which time the nodal line had rotated through an angle of 7° . The values of Ω shown in figure 10 are the values at the beginning of the tracking period. Again 26 range and 26 range-rate observations were assumed to have been made during each orbit, with the elements other than Ω being held at the nominal values. For the elliptic orbit in the present investigation, it was found that the elements Ω , ω , and e are best determined when the orbit is viewed on edge ($\Omega = 0^\circ$ and 180°) whereas the elements a , i , and t_0 are best determined when the orbit is viewed broadside ($\Omega = 90^\circ$ and 270°). The very large variation in the curve for σ_i is due to the fact that, as stated earlier, the partial derivatives of range and range rate with respect to i are approximately proportional to $\sin \Omega$. As Ω approaches 90° and 270° , the amplitudes of these derivatives approach the maximum values, and therefore the inclination is more accurately determined at these nodal positions. The curves in figure 10 show a periodic property with a period equal to 1 lunar month. They are also symmetric about 90° and 180° because occultation was not considered. If occultation had been considered, this symmetry would have been partially destroyed. In the discussion of figures 2 and 3 it was stated that $\partial \rho / \partial \Omega$ is approximately equal to $\partial \rho / \partial \omega$ and that $\partial \dot{\rho} / \partial \Omega$ is approximately equal to $\partial \dot{\rho} / \partial \omega$ for near-zero inclinations. Therefore for small inclinations, high correlations between Ω and ω and a similar accuracy of estimation would be expected. It can be seen in figure 10 that even with a medium inclination, the curves for σ_Ω and σ_ω are very much alike with approximately the same variations. The correlation coefficient after five orbits is 0.9985. It can also be seen in figure 10 that the relative advantage of one data type over the other is not constant over the range of nodal positions in the investigation but remains within a factor of approximately 2.

The effect of eccentricity upon the accuracy of estimating the elements is illustrated in figure 11. It was assumed that the elements i , Ω , ω , and t_0 were held constant at the nominal values while the semimajor axis was fixed at 5000 kilometers and e was varied between 0.01 and 0.6. The results shown are those obtained by assuming that the satellite was tracked over a period of five consecutive orbits with 26 range and 26 range-rate observations made per orbit. Except for the accuracy of estimating e which had only a slight variation, the accuracy of estimating the elements was found to increase as the eccentricity increased. However, it can be seen that for eccentricities above 0.1 the accuracy of determining the orientation angles i , Ω , and ω is not appreciably improved when e increases whereas the scale of the orbit, which is inferred by the semimajor axis a , improves significantly. The results indicate that the accuracy of estimating the time of periapsis passage t_0 is very dependent upon the eccentricity. Since the position in orbit is dependent

upon t_0 and, furthermore, since the knowledge of t_0 greatly improves with an increase in eccentricity, it can be concluded that the position in orbit is better determined at the higher eccentricities. It should also be noted that the data presented in figure 11 seem to indicate that range measurements are better than range-rate measurements for all values of e ; however, it must be remembered that in this case the semimajor axis is fixed at 5000 kilometers and that, as noted previously, range data have a definite advantage over range-rate data for large values of a . Hence, it should not be concluded that range measurements are always better than range-rate measurements for all values of e . However, it can be concluded that for the elements a and t_0 the relative advantage of one data type over the other is somewhat dependent upon e . As shown in the following paragraph, the accuracy of determining the position of a satellite in orbit is primarily limited by the accuracy of determining the orientation angles, and it can be seen from figure 11 that the relative advantage of one data type over the other for determining these angles is independent of e . Therefore it can also be concluded that in the determination of the position of a satellite, the relative advantage of one data type over the other is independent of e .

One of the more important parameters to be estimated in any orbit-determination problem is the position of the satellite. It is therefore of interest to know how accurately this position can be determined. A qualitative expression for the accuracy of determining the position in terms of the one-sigma errors in the estimates of the elements can be obtained as follows. The vector \bar{r} is written as

$$\bar{r} = \bar{r}(a, i, \Omega, \omega, e, t_0, t) \quad (10)$$

and therefore at some fixed time

$$\Delta\bar{r} = \frac{\partial\bar{r}}{\partial a} \Delta a + \frac{\partial\bar{r}}{\partial i} \Delta i + \frac{\partial\bar{r}}{\partial \Omega} \Delta \Omega + \frac{\partial\bar{r}}{\partial \omega} \Delta \omega + \frac{\partial\bar{r}}{\partial e} \Delta e + \frac{\partial\bar{r}}{\partial t_0} \Delta t_0 \quad (11)$$

Equation (11) is then put into rectangular (x, y, z) component form where the partial derivatives of x , y , and z with respect to the orbital elements are maximized with respect to the position in orbit and the angular variables i , Ω , and ω . By using the triangle inequality, the length of the vector $\Delta\bar{r}$ can be written as

$$|\Delta\bar{r}| \leq |\Delta x| + |\Delta y| + |\Delta z| \quad (12)$$

The maximized partial derivatives can then be substituted into the relation given in inequality (12) and if the largest coefficient of each incremental change in the elements from the three-component inequality is selected, the following equation can be written:

$$|\Delta \bar{r}| \leq 3 \left[(1 + e)\Delta a + a(1 + e)(\Delta i + \Delta \Omega + \Delta \omega) + \left(\frac{2a}{1 - e^2} \right) (3 \Delta e + n \Delta t_0) \right] \quad (13)$$

By assuming that the small incremental changes in the elements are equal to the standard deviations of the elements and that $|\Delta \bar{r}|$ is equal to the standard deviation of the position P, inequality (13) can be written as

$$\sigma_P \leq 3 \left[(1 + e)\sigma_a + a(1 + e)(\sigma_i + \sigma_\Omega + \sigma_\omega) + \left(\frac{2a}{1 - e^2} \right) (3\sigma_e + n\sigma_{t_0}) \right] \quad (14)$$

It can be shown by substituting the one-sigma errors in the estimates of the elements from figure 4 into inequality (14) that the major contribution to the uncertainty in the position is the uncertainty in the orientation angles. Hence, it is very important to make measurements which allow an accurate determination of these angles in order that the position of the satellite might be determined with the most accuracy.

Another point of interest, which is also noted in reference 3, is that the reflection of any given orbit through the earth-moon plane would give the same time history for range and range-rate measurements as that of the original orbit. This fact implies that an addition of 180° to both the node and the argument of periapsis would not result in any change in the accuracy of determining the elements and that without a priori information it would not be known which of the two orbits was being tracked.

CONCLUDING REMARKS

A parametric study of the effects of tracking mode and orbital parameters on the accuracy of determining the state of a lunar satellite has been made by using range and range-rate measurements. A comparison of the relative advantage of using either range or range-rate measurements indicates that the advantage of one data type over the other is very dependent on the semimajor axis and somewhat dependent on the nodal position and eccentricity but is not dependent on the inclination. For lunar orbits with medium eccentricity and with semimajor axes of approximately 2500 kilometers, the orbital elements could be determined with equal accuracy by using either range or range-rate data when the ratio of the standard deviation of range measurements to the standard deviation of range-rate measurements was approximately 1500 seconds. For lunar orbits with semimajor axis smaller than approximately 2500 kilometers, range-rate measurements gave a more accurate determination of the elements, whereas for orbits with semimajor axes greater than approximately 2500 kilometers, range measurements proved to be the better data type of the two. It was concluded that range and range-rate measurements are similar data types in that they produce similar correlation matrices for the state variables and simultaneous

use of both data types does not significantly reduce correlations between the elements.

Langley Research Center,
National Aeronautics and Space Administration,
Langley Station, Hampton, Va., October 11, 1965.

APPENDIX A

DETAILS OF WEIGHTED LEAST SQUARES SIMULATION

A special case of a weighted least squares process was used in the error analysis presented in this report. This appendix is included to illustrate the basic equations which were used in the IBM 709⁴ electronic data processing system. In particular, the method of obtaining the covariance matrix of the orbital elements is shown. This method is essentially the same as that described in reference 4.

The solution of the equations of motion of a point mass about a central body contains six constants of the motion which may be taken as a , i , Ω , ω , e , and t_0 . The observable quantities, range and range rate, written as functions of these six constants at any given time t are

$$\left. \begin{aligned} \rho &= f(a, i, \Omega, \omega, e, t_0, t) \\ \dot{\rho} &= F(a, i, \Omega, \omega, e, t_0, t) \end{aligned} \right\} \quad (A1)$$

Theoretically only six properly chosen measurements would be required to determine the six elements of equations (A1) provided there were no errors in the measurements. Since a measurement error ϵ_i is associated with any measurement ρ_i or $\dot{\rho}_i$, more than six measurements can be used to obtain a "best" set of elements. The notion of "best" is to be defined subsequently. The subscript i denotes the i th measurement.

Equations (A1) represent the functional equations for range and range rate but similar representation can be made for any measurable quantity. The following equation can be written for the i th measurement of the general quantity y and error in the i th measurement ϵ_i :

$$y_i = f_i(\alpha_j, t_i) + \epsilon_i \quad (A2)$$

In equation (A2), y_i is analogous to the i th measurement of range or range rate (defined in eq. (A1)) whereas α_j is analogous to the elements in equation (A1). In general, f is a nonlinear function in the α_j 's, and in order to make the problem amenable to solution, the basic equations are linearized about a nominal set α_j^0 . If the true values of α_j are assumed to be close to a nominal set α_j^0 , then $y^0(t_i) = y_i^0 = f(\alpha_j^0, t_i)$ where y_i^0 is the calculated value of the i th measurement obtained by using the nominal set α_j^0 . The following equation can then be written:

APPENDIX A

$$\Delta y_i = y_i - y_i^o = f(\alpha_j, t_i) - f(\alpha_j^o, t_i) + \epsilon_i \quad (A3)$$

If equation (A3) is expanded in a Taylor series about the nominal set α_j^o and if the terms of order higher than the first are dropped, the following equation is obtained:

$$\Delta y_i = \left. \frac{\partial f(t_i)}{\partial \alpha_1} \right|_o (\alpha_1 - \alpha_1^o) + \dots + \left. \frac{\partial f(t_i)}{\partial \alpha_j} \right|_o (\alpha_j - \alpha_j^o) + \epsilon_i \quad (A4)$$

The notation $\left. \frac{\partial f(t_i)}{\partial \alpha_j} \right|_o$ means the partial derivative of $f(\alpha_k, t_i)$ with respect to the j th element evaluated at the prescribed set α_j^o , $j = 1, 2, \dots, 6$, at the time t_i . By denoting $(\alpha_j - \alpha_j^o) = \Delta \alpha_j$, equation (A4) can be written as

$$\Delta y_i = \sum_{j=1}^6 \left. \frac{\partial f(t_i)}{\partial \alpha_j} \right|_o \Delta \alpha_j + \epsilon_i \quad (A5)$$

Equation (A5) can be written in matrix form as

$$\Delta y = A \Delta \alpha + \epsilon \quad (A6)$$

where Δy is an $N \times 1$ column vector of the observed minus the computed values of y , A is an $N \times 6$ matrix of known partial derivatives, $\Delta \alpha$ is a 6×1 column vector of deviations of the elements from the nominal set, and ϵ is an $N \times 1$ column vector of observation errors. The problem is to find the best estimate $\hat{\Delta \alpha}$ of $\Delta \alpha$ when Δy and A are given. If $\hat{\Delta \alpha}$ is determined and the nominal values α^o are used, the best estimate of α is $\hat{\alpha} = \alpha^o + \hat{\Delta \alpha}$.

In order to specify what is meant by best estimate, some quantities must first be defined. Denote $\hat{\alpha}$ as the best estimate for α , $\hat{y} = A\hat{\alpha}$ as the best estimate of the true value of the observable, and $y - \hat{y} = y - A\hat{\alpha} = \hat{\epsilon}$ as the best estimate of the observation error. Note that the deltas have been dropped to simplify notation.

The best estimate of α is now defined as that α which minimizes the sum of the squares of the weighted components of the residual vector $y - A\hat{\alpha}$.

APPENDIX A

In order to account for the difference in confidence between various observations and the possible relations between them, a so-called weighting matrix W which is assumed to be a symmetric, positive-definite $N \times N$ matrix is introduced. The weighted least squares function which is to be minimized can now be written as

$$Q(\alpha) = (y - A\alpha)^T W (y - A\alpha) = \epsilon^T W \epsilon \quad (A7)$$

In order to minimize the function in equation (A7), the variational principle given in reference 4 is used. This principle states that in order for Q to be an extremum, the first variation in Q must vanish and in order for this extremum to be a minimum, the second variation must be positive-definite. If this principle is applied, with only the variation in α being considered, the following equation can be written:

$$\begin{aligned} \delta Q &= -\delta\alpha^T A^T W (y - A\alpha) - (y - A\alpha)^T W A \delta\alpha \\ &= -2\delta\alpha^T A^T W (y - A\alpha) \end{aligned} \quad (A8)$$

The value of this equation must be zero for an extremum, and the fact that $\delta\alpha$ is arbitrary implies that the best estimate $\hat{\alpha}$ must satisfy the equation

$$A^T W (y - A\hat{\alpha}) = 0 \quad (A9)$$

or

$$A^T W A \hat{\alpha} = A^T W y \quad (A10)$$

Premultiplying both sides of equation (A10) by $(A^T W A)^{-1}$ gives the best estimate

$$\hat{\alpha} = (A^T W A)^{-1} A^T W y \quad (A11)$$

provided $A^T W A$ is nonsingular. In order to show that this is the α which minimizes Q , it is sufficient to show that the second variation is positive-definite, where the second variation is

$$\delta^2 Q = 2\delta\alpha^T A^T W A \delta\alpha \quad (A12)$$

For arbitrary $\delta\alpha$, equation (A12) is greater than zero if W is positive-definite. One of the basic assumptions was that W is positive-definite, and therefore $\hat{\alpha}$ in equation (A11) is the best estimate of α .

APPENDIX A

The remainder of this appendix is devoted to the development of the covariance matrix. Equation (A11) has been used to determine the best estimate $\hat{\alpha}$ and it is now desirable to determine the statistics of $\hat{\alpha}$. For example, how well was α estimated? The definitions of the variance and the first mixed moment can be used to write that the covariance matrix for $\hat{\alpha}$ is $E(\hat{\alpha}\hat{\alpha}^T)$ where E denotes the expected value of the variable in the parentheses. By use of equation (A11), the following equation can be written:

$$E(\hat{\alpha}\hat{\alpha}^T) = E\left[\left(A^TWA\right)^{-1}A^TWyy^TW^TA\left(A^TW^TA\right)^{-1}\right] \quad (A13)$$

Since all terms except the random variable y are constant in equation (A13), the operator E operates only on y and y^T . Hence,

$$E(\hat{\alpha}\hat{\alpha}^T) = \left(A^TWA\right)^{-1}A^TWE\left(yy^T\right)W^TA\left(A^TW^TA\right)^{-1} \quad (A14)$$

Reference 4 shows that the best choice of W is the inverse of the covariance matrix for the measurements where this covariance matrix is $E(yy^T)$. Assume that each measurement is of equal weight (i.e., $\sigma_{y_1}^2 = \sigma_{y_2}^2 = \dots = \sigma_{y_N}^2$) and that the observations or measurements are completely uncorrelated. If these assumptions are made and if it is noted that $E(yy^T)$ is the covariance matrix for the measurements, then

$$W = \left[E\left(yy^T\right)\right]^{-1} = \frac{1}{\sigma_{y_1}^2} I \quad (A15)$$

and

$$WE\left(yy^T\right) = I \quad (A16)$$

where I is the identity matrix. Hence, equation (A14) becomes

$$\begin{aligned} \Lambda_{\hat{\alpha}} &= E(\hat{\alpha}\hat{\alpha}^T) = \left(A^TWA\right)^{-1}\left(A^TW^TA\right)\left(A^TW^TA\right)^{-1} \\ &= \left(A^TWA\right)^{-1} = \sigma_y^2\left(A^TA\right)^{-1} \end{aligned} \quad (A17)$$

APPENDIX A

Note that in the terms of the orbital elements

$$\Lambda_{\hat{\alpha}} = \begin{bmatrix} \sigma_a^2 & \rho_{ai}\sigma_a\sigma_i & \rho_{a\Omega}\sigma_a\sigma_\Omega & \rho_{a\omega}\sigma_a\sigma_\omega & \rho_{ae}\sigma_a\sigma_e & \rho_{at_o}\sigma_a\sigma_{t_o} \\ \rho_{ia}\sigma_i\sigma_a & \sigma_i^2 & \rho_{i\Omega}\sigma_i\sigma_\Omega & \rho_{i\omega}\sigma_i\sigma_\omega & \rho_{ie}\sigma_i\sigma_e & \rho_{it_o}\sigma_i\sigma_{t_o} \\ \rho_{\Omega a}\sigma_\Omega\sigma_a & \rho_{\Omega i}\sigma_\Omega\sigma_i & \sigma_\Omega^2 & \rho_{\Omega\omega}\sigma_\Omega\sigma_\omega & \rho_{\Omega e}\sigma_\Omega\sigma_e & \rho_{\Omega t_o}\sigma_\Omega\sigma_{t_o} \\ \rho_{\omega a}\sigma_\omega\sigma_a & \rho_{\omega i}\sigma_\omega\sigma_i & \rho_{\omega\Omega}\sigma_\omega\sigma_\Omega & \sigma_\omega^2 & \rho_{\omega e}\sigma_\omega\sigma_e & \rho_{\omega t_o}\sigma_\omega\sigma_{t_o} \\ \rho_{ea}\sigma_e\sigma_a & \rho_{ei}\sigma_e\sigma_i & \rho_{e\Omega}\sigma_e\sigma_\Omega & \rho_{e\omega}\sigma_e\sigma_\omega & \sigma_e^2 & \rho_{et_o}\sigma_e\sigma_{t_o} \\ \rho_{t_o a}\sigma_{t_o}\sigma_a & \rho_{t_o i}\sigma_{t_o}\sigma_i & \rho_{t_o\Omega}\sigma_{t_o}\sigma_\Omega & \rho_{t_o\omega}\sigma_{t_o}\sigma_\omega & \rho_{t_o e}\sigma_{t_o}\sigma_e & \sigma_{t_o}^2 \end{bmatrix} = \left(A^T W A \right)^{-1} = \sigma_y^2 \left(A^T A \right)^{-1} \quad (A18)$$

where $\rho_{ai}\sigma_a\sigma_i$, $\rho_{a\Omega}\sigma_a\sigma_\Omega$, and so forth, are the first mixed moments and ρ_{ai} , $\rho_{a\Omega}$, and so forth, are the correlation coefficients. This matrix was used to obtain the results in the present report. It can be seen from equation (A17) that no actual measurements are needed to determine the variances of the elements; in particular, only the variance of the measurements is needed. The covariance matrix for the simultaneous use of two data types such as range and range rate can be written in several ways, one of which is

$$\Lambda_{\hat{\alpha}} = \left[\frac{A^T A}{\sigma_\rho^2} + \frac{B^T B}{\sigma_{\dot{\rho}}^2} \right]^{-1}$$

The correlation matrix is a matrix having ones as the diagonal terms and the correlation coefficients of equations (A18) as the off-diagonal terms.

It should be remembered that equation (A17) is a special case of the generalized weighted least squares as given in equation (A13). From the special form given in equation (A17), it can be seen that for a single data type the variances of the elements are proportional to the variance of the measurements.

APPENDIX B

EQUATIONS FOR PARTIAL DERIVATIVES OF RANGE AND RANGE RATE
WITH RESPECT TO ORBITAL ELEMENTS

The elements of the A matrix which are the partial derivatives of range and range rate with respect to the orbital elements are as follows:

$$\frac{\partial \rho}{\partial a} = \frac{1}{\rho} \left\{ (r + Rl_1) \left[\frac{r}{a} - \frac{3ae}{2r} n(t - t_0) \sin E \right] - \frac{3}{2} Rl_2 \frac{a}{r} n(t - t_0) (1 - e^2)^{1/2} \right\} \quad (B1)$$

$$\frac{\partial \rho}{\partial i} = \frac{1}{\rho} Rrn_1 \sin \Omega \quad (B2)$$

$$\frac{\partial \rho}{\partial \Omega} = - \frac{1}{\rho} Rrm_1 \quad (B3)$$

$$\frac{\partial \rho}{\partial \omega} = \frac{1}{\rho} Rrl_2 \quad (B4)$$

$$\begin{aligned} \frac{\partial \rho}{\partial e} = \frac{1}{\rho} \left\{ a(r + Rl_1) \left[\left(\frac{a}{r} \right) e \sin^2 E - \cos E \right] \right. \\ \left. + Rrl_2 \left(\frac{a}{r} \right)^2 \left[\frac{r}{a} \frac{\sin E}{(1 - e^2)^{1/2}} + (1 - e^2)^{1/2} \sin E \right] \right\} \quad (B5) \end{aligned}$$

$$\frac{\partial \rho}{\partial t_0} = - \frac{n}{\rho} \left[\frac{a^2}{r} (r + Rl_1) e \sin E + Rl_2 \frac{a^2}{r} (1 - e^2)^{1/2} \right] \quad (B6)$$

APPENDIX B

$$\begin{aligned}
\frac{\partial \dot{\rho}}{\partial a} &= \frac{1}{\rho} \left\{ -\dot{\rho} \frac{\partial \rho}{\partial a} + \xi R \left(r \frac{\partial m_1}{\partial a} + m_1 \frac{\partial r}{\partial a} \right) + \sqrt{a\mu} \frac{\partial}{\partial a} (E - M) + \sqrt{\frac{\mu}{a}} \frac{(E - M)}{2} \right. \\
&\quad + R \frac{\sqrt{a\mu}}{r} \left[l_1 \frac{\partial}{\partial a} (E - M) + (E - M) \frac{\partial l_1}{\partial a} + (1 - e^2)^{1/2} \frac{\partial l_2}{\partial a} \right] \\
&\quad \left. + R \left[l_1 (E - M) + l_2 (1 - e^2)^{1/2} \right] \left(\frac{1}{2r} \sqrt{\frac{\mu}{a}} - \frac{1}{r^2} \sqrt{a\mu} \frac{\partial r}{\partial a} \right) \right\} \quad (B7)
\end{aligned}$$

$$\frac{\partial \dot{\rho}}{\partial i} = \frac{1}{\rho} \left\{ -\dot{\rho} \frac{\partial \rho}{\partial i} - \xi R r m_1 \cos \Omega + \frac{R}{r} \sqrt{a\mu} \sin \Omega \left[n_1 (E - M) + n_2 (1 - e^2)^{1/2} \right] \right\} \quad (B8)$$

$$\frac{\partial \dot{\rho}}{\partial \Omega} = \frac{1}{\rho} \left\{ -\dot{\rho} \frac{\partial \rho}{\partial \Omega} + \xi R r l_1 - \frac{R}{r} \sqrt{a\mu} \left[m_1 (E - M) + m_2 (1 - e^2)^{1/2} \right] \right\} \quad (B9)$$

$$\frac{\partial \dot{\rho}}{\partial \omega} = \frac{1}{\rho} \left\{ -\dot{\rho} \frac{\partial \rho}{\partial \omega} + \xi R r m_2 + \frac{R}{r} \sqrt{a\mu} \left[l_2 (E - M) - l_1 (1 - e^2)^{1/2} \right] \right\} \quad (B10)$$

$$\begin{aligned}
\frac{\partial \dot{\rho}}{\partial e} &= \frac{1}{\rho} \left(-\dot{\rho} \frac{\partial \rho}{\partial e} + \left\{ \xi R m_1 - \frac{R}{r^2} \sqrt{a\mu} \left[l_1 (E - M) + l_2 (1 - e^2)^{1/2} \right] \right\} \left(\frac{a^2}{r} e \sin^2 E - a \cos E \right) + \frac{\sqrt{a\mu}}{r^2} a (r + R l_1) \sin E \right. \\
&\quad \left. - \frac{\sqrt{a\mu}}{r} R l_2 e (1 - e^2)^{-1/2} + \left\{ \xi R m_2 + \frac{R}{r} \sqrt{a\mu} \left[l_2 (E - M) - l_1 (1 - e^2)^{1/2} \right] \right\} \left[(1 - e^2)^{-1/2} + \frac{a}{r} (1 - e^2)^{1/2} \right] \frac{a}{r} \sin E \right) \quad (B11)
\end{aligned}$$

$$\begin{aligned}
\frac{\partial \dot{\rho}}{\partial t_o} &= \frac{n}{\rho} \left(-\dot{\rho} \frac{\partial \rho}{\partial t_o} - \left\{ \xi R m_1 - \frac{R}{r^2} \sqrt{a\mu} \left[l_1 (E - M) + l_2 (1 - e^2)^{1/2} \right] \right\} \frac{a^2}{r} e \sin E - \frac{\sqrt{a\mu}}{r^2} (r + R l_1) a e \cos E \right. \\
&\quad \left. - \left\{ \xi R m_2 + \frac{R}{r} \sqrt{a\mu} \left[l_2 (E - M) - l_1 (1 - e^2)^{1/2} \right] \right\} \left[\left(\frac{a}{r} \right)^2 (1 - e^2)^{1/2} \right] \right) \quad (B12)
\end{aligned}$$

APPENDIX B

where

$$\rho^2 = R^2 + r^2 + 2Rr\iota_1$$

$$\dot{\rho} = -\xi \frac{\partial \rho}{\partial \Omega} - \frac{\partial \rho}{\partial t_0}$$

$$\frac{\partial r}{\partial a} = \frac{r}{a} - \frac{3}{2} \frac{ae}{r} n(t - t_0) \sin E$$

$$\frac{\partial}{\partial a}(E - M) = -\frac{3}{2} n(t - t_0) \frac{e}{r} \cos E$$

$$\frac{\partial \iota_1}{\partial a} = -\frac{3}{2} \frac{a}{r^2} \iota_2 n(t - t_0) (1 - e^2)^{1/2}$$

$$\frac{\partial m_1}{\partial a} = -\frac{3}{2} \frac{a}{r^2} m_2 n(t - t_0) (1 - e^2)^{1/2}$$

$$\frac{\partial \iota_2}{\partial a} = \frac{3}{2} \frac{a}{r^2} \iota_1 n(t - t_0) (1 - e^2)^{1/2}$$

In the equations in this appendix a , i , Ω , ω , e , and t_0 are the conventional Keplerian elements. The mean anomaly M is given by Kepler's equation

$$M = n(t - t_0) = E - e \sin E$$

where n is the mean angular rate of the satellite.

The direction cosines are as follows:

$$\iota_1 = \cos \theta \cos \Omega - \sin \theta \sin \Omega \cos i$$

$$\iota_2 = -\sin \theta \cos \Omega - \cos \theta \sin \Omega \cos i$$

$$m_1 = \cos \theta \sin \Omega + \sin \theta \cos \Omega \cos i$$

$$m_2 = -\sin \theta \sin \Omega + \cos \theta \cos \Omega \cos i$$

$$n_1 = \sin \theta \sin i$$

$$n_2 = \cos \theta \sin i$$

REFERENCES

1. Lorell, J.; Anderson, J. D.; and Sjogren, W. L.: Characteristics and Format of the Tracking Data to Be Obtained by the NASA Deep Space Instrumentation Facility for Lunar Orbiter. Tech. Mem. No. 33-230 (Contract No. NAS 7-100), Jet Propulsion Lab., California Inst. Technol., June 15, 1965.
2. Lorell, Jack: Orbit Determination for a Lunar Satellite. J. Astronaut. Sci., vol. XI, no. 1, 1964, pp. 1-7.
3. Gates, C. R., ed.: The Behavior of Lunar Satellites and the Determination of Their Orbits: A Preliminary Investigation. Tech. Mem. No. 33-107 (Contract No. NAS 7-100), Jet Propulsion Lab., California Inst. Technol., Sept. 18, 1962.
4. Solloway, C. B.: Elements of the Theory of Orbit Determination. EPD-255 (Contract No. NAS 7-100), Jet Propulsion Lab., California Inst. Technol., Dec. 9, 1964.

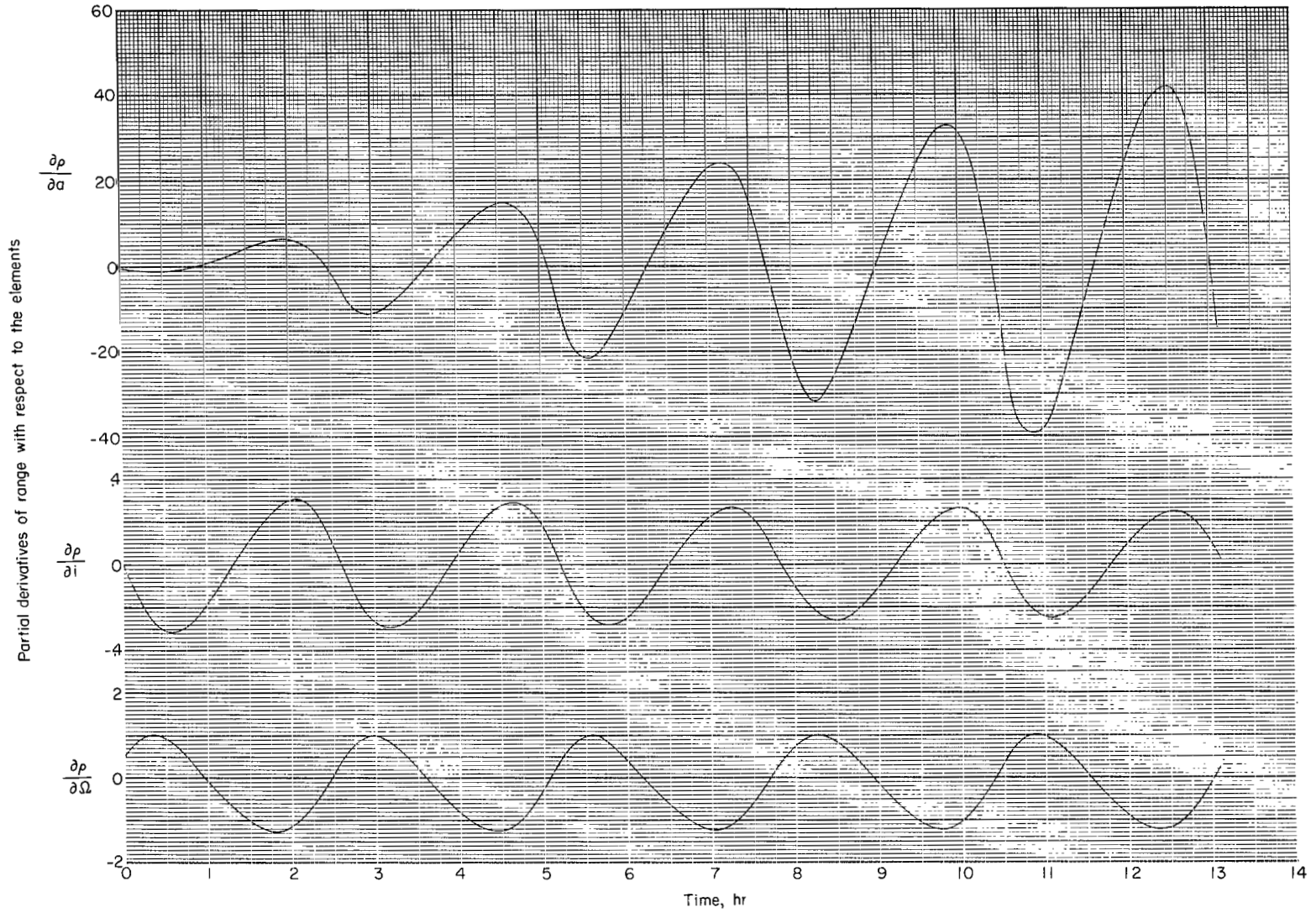


Figure 2.- Variation with time of the partial derivatives of range with respect to the elements.

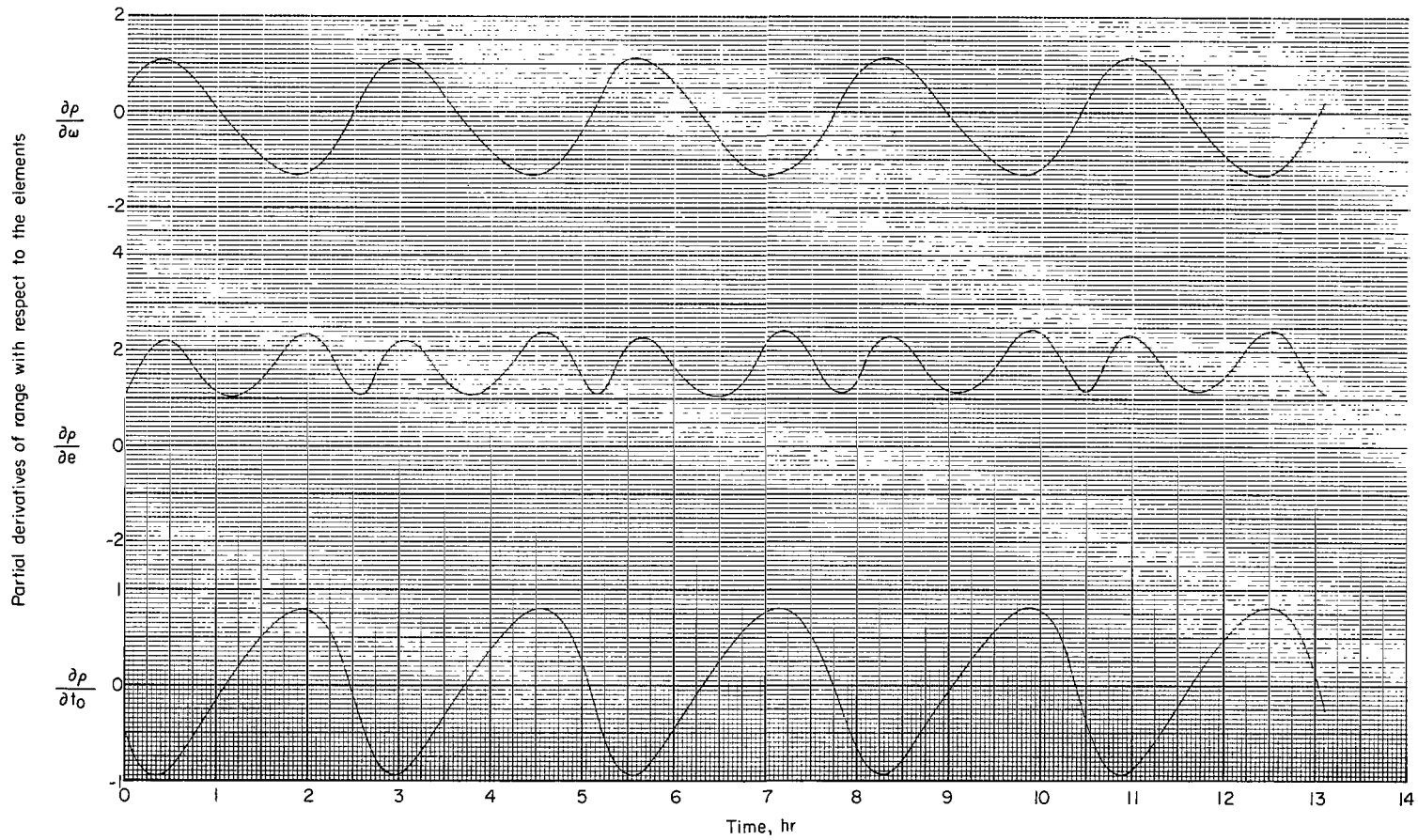


Figure 2.- Concluded.

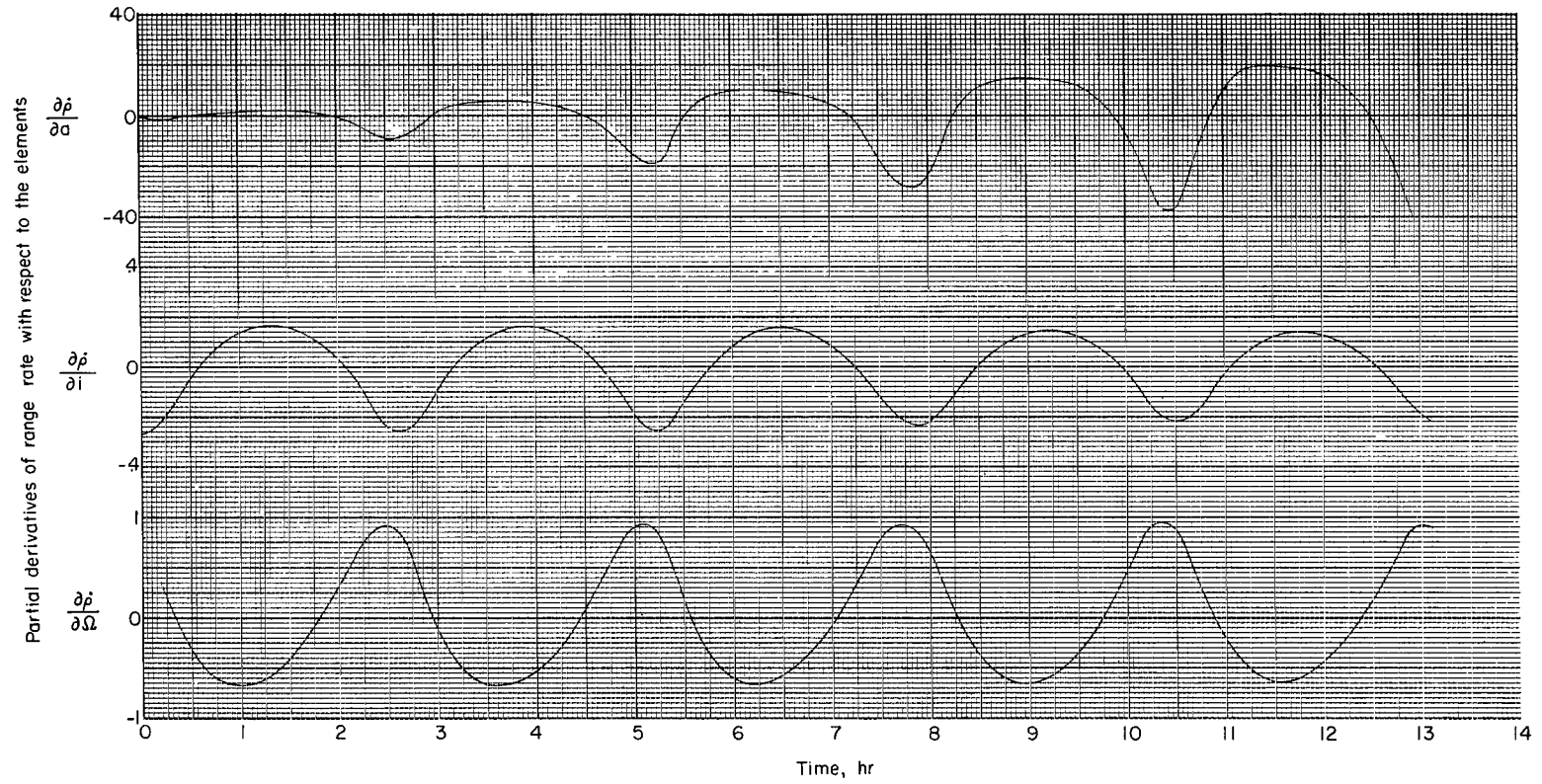


Figure 3.- Variation with time of the partial derivatives of range rate with respect to the elements.

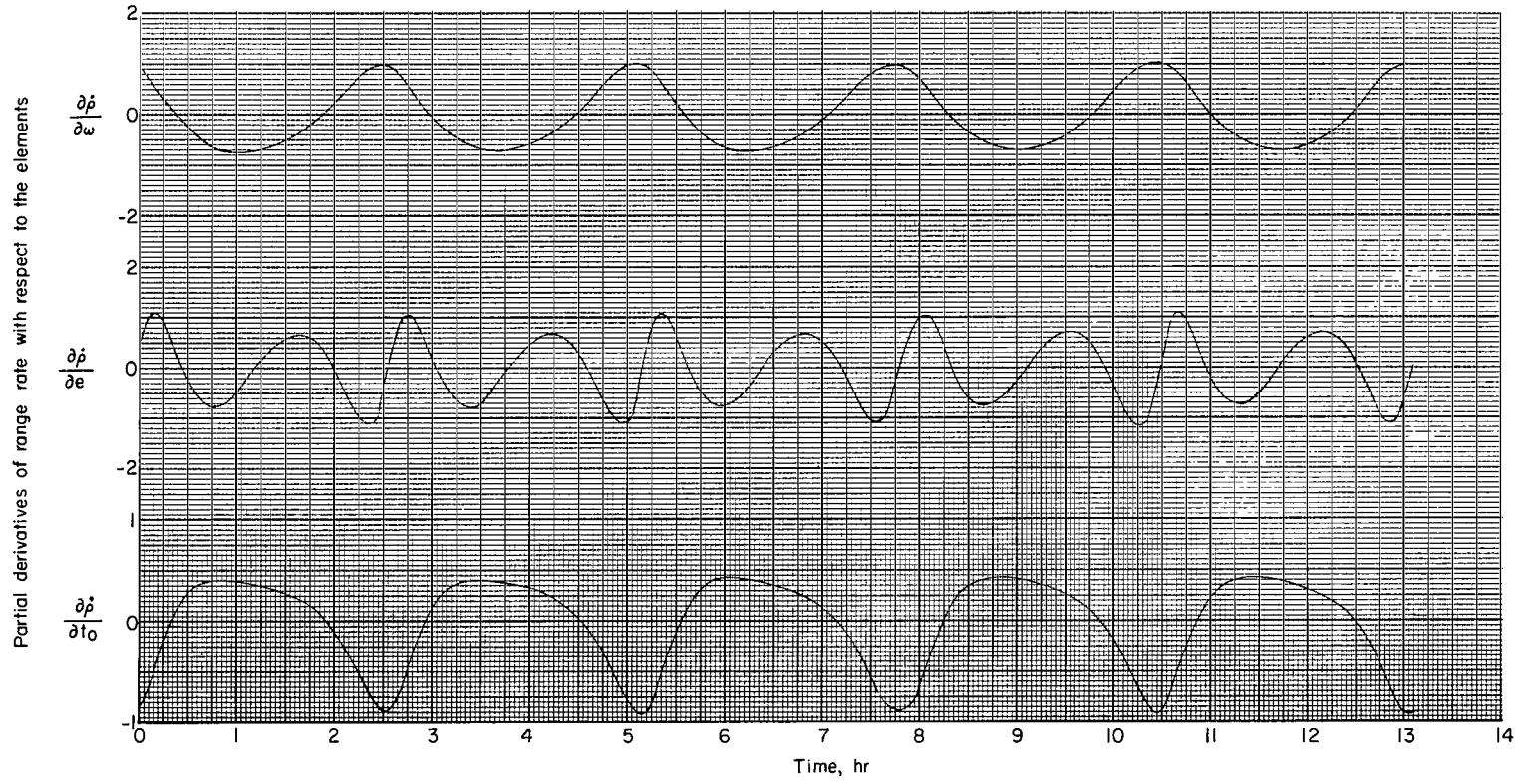


Figure 3.- Concluded.

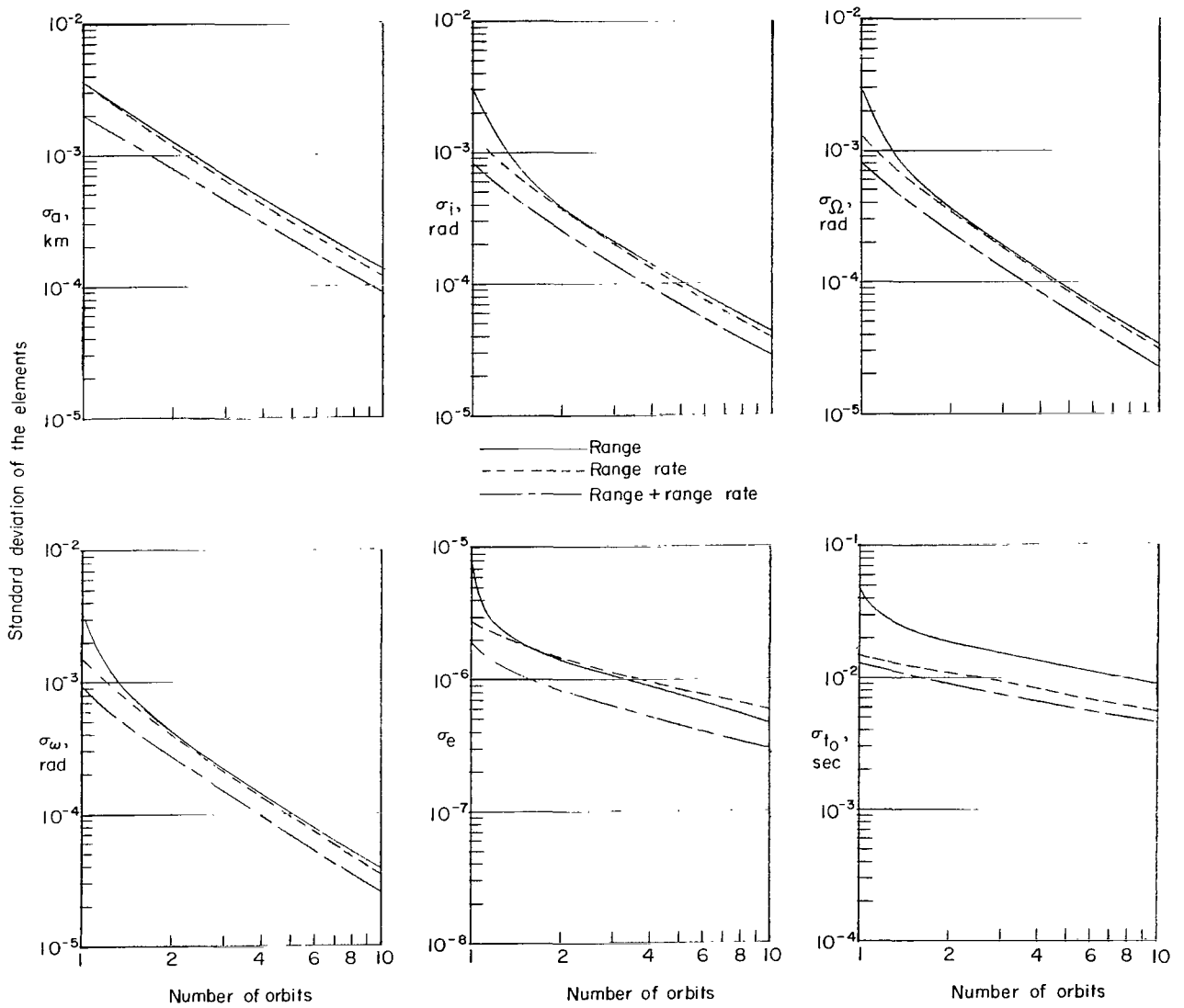


Figure 4.- Variation of the standard deviation of the nominal-orbital elements with the number of orbits assumed to have been tracked.

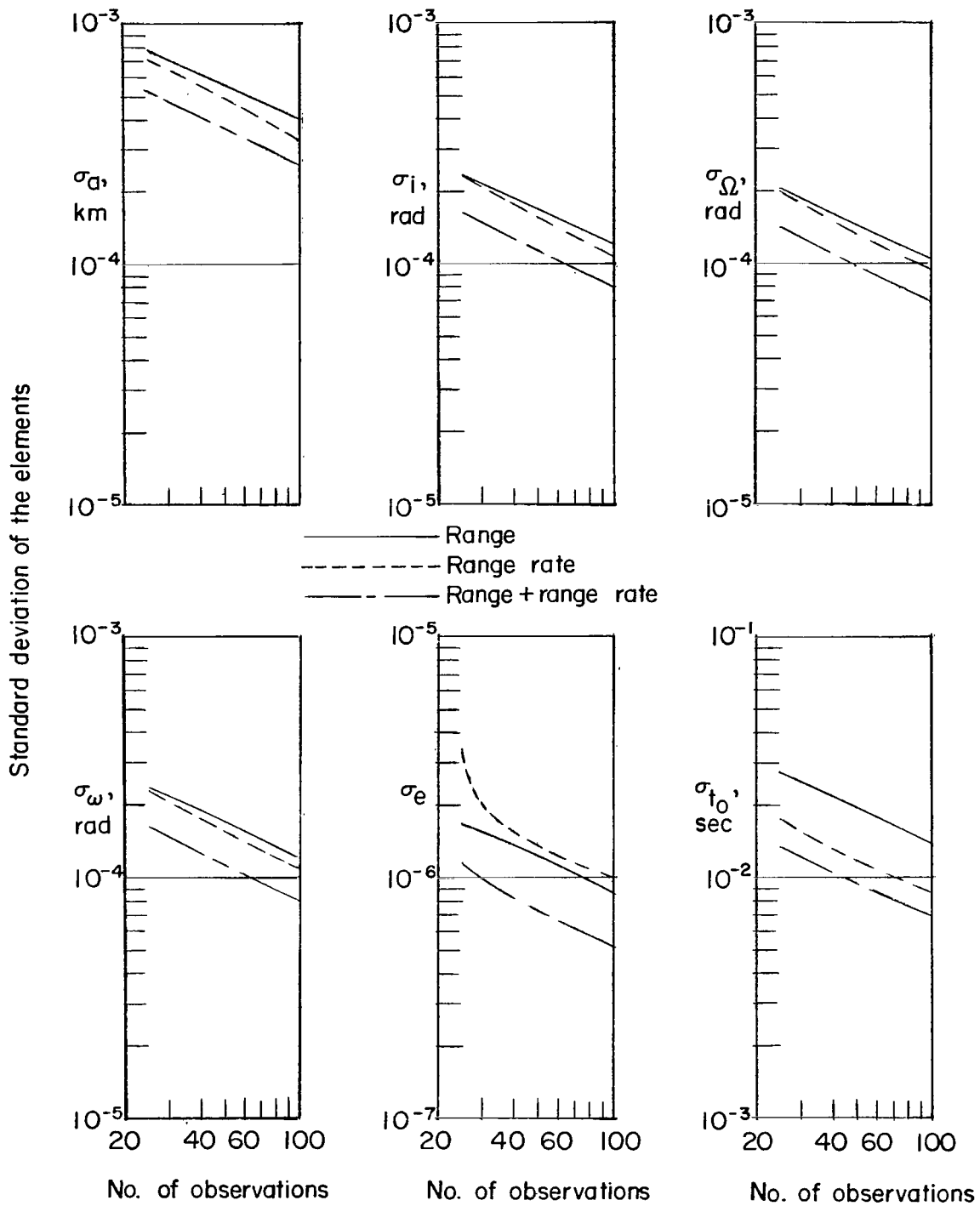


Figure 5.- Variation of the standard deviation of the nominal-orbit elements with the number of observations. The observations were assumed to have been made over five orbits.

Elements		a	i	Ω	ω	e	t_0
Elements	a	1	.44784	-.44659	.44710	.23886	.24076
	i		1	-.99998	.99997	.95278	.82696
	Ω			1	-.99998	-.95307	-.82769
	ω				1	.95387	.83023
	e					1	.91737
	t_0						1

		a	i	Ω	ω	e	t_0
	a	1	.92076	-.92101	.92076	.25836	-.15214
	i		1	-.99992	.99992	.50851	.01002
	Ω			1	-.99998	-.50770	-.01039
	ω				1	.50824	.01620
	e					1	.24235
	t_0						1

		a	i	Ω	ω	e	t_0
	a	1	.79610	-.79579	.79495	.24406	-.07346
	i		1	-.99989	.99988	.68057	.24239
	Ω			1	-.99996	-.67996	-.24400
	ω				1	.68324	.25147
	e					1	.62880
	t_0						1

Figure 6.- Correlation matrices after one orbit.

Elements		a	i	Ω	ω	e	t_0
Elements	a	1	.9077	-.9055	.9038	.0566	-.3059
	i		1	-.9958	.9937	.1109	-.2611
	Ω			1	-.9971	-.1078	.2468
	ω				1	.1693	-.1772
	e					1	.7471
	t_0	Range					

a	i	Ω	ω	e	t_0	
1	.9063	-.9047	.9045	-.0198	-.5873	
	1	-.9951	.9958	.0549	-.5111	
		1	-.9988	-.0499	.5063	
			1	.0522	-.4715	
				1	.0371	
Range rate						1

a	i	Ω	ω	e	t_0	
1	.9051	-.9033	.9023	-.0134	-.5261	
	1	-.9954	.9955	.0644	-.4527	
		1	-.9986	-.0529	.4436	
			1	.0809	-.4019	
				1	.4294	
Range + range rate						1

Figure 7.- Correlation matrices after five orbits.

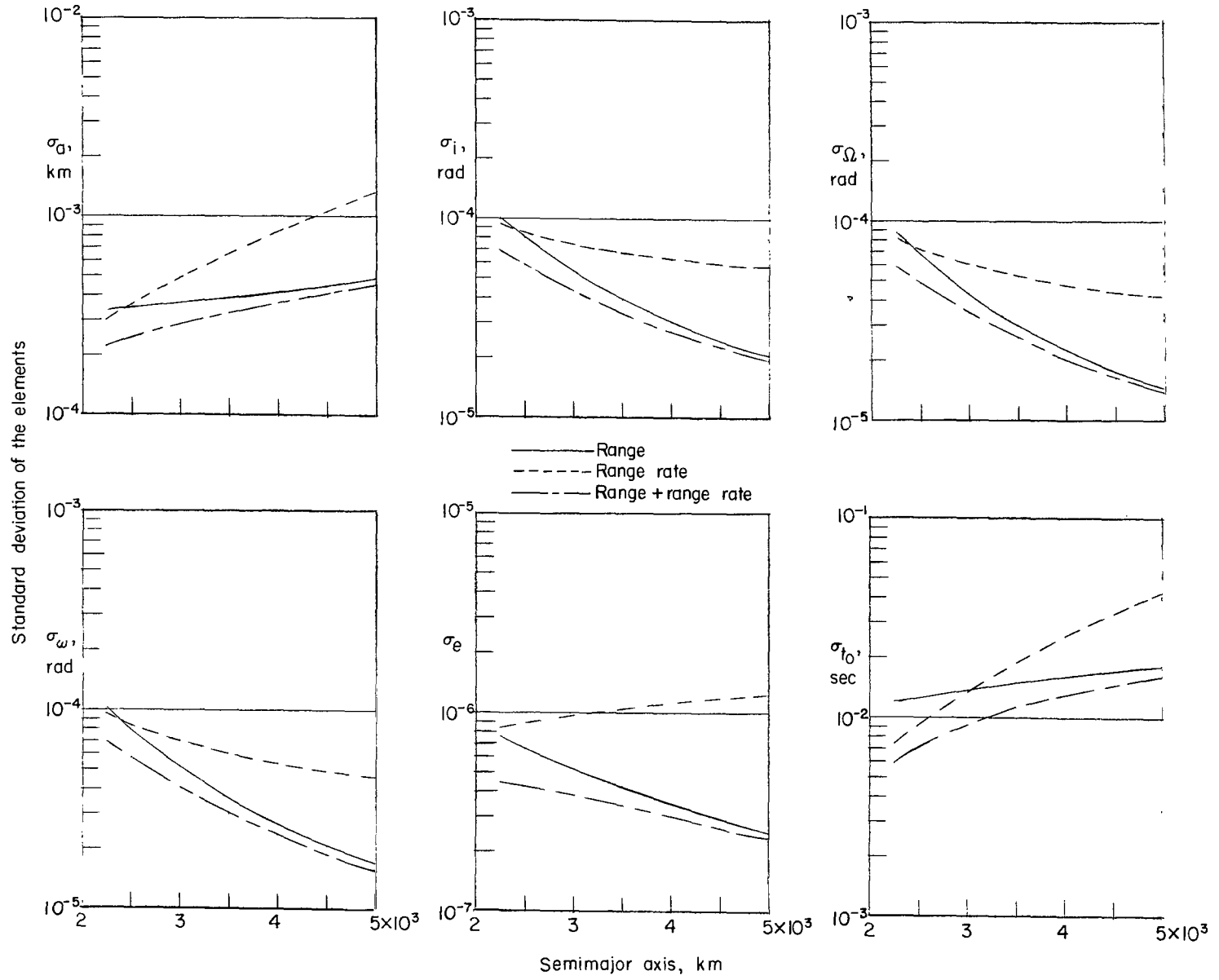


Figure 8.- Variation of the standard deviation of the nominal-orbit elements with the semimajor axis.

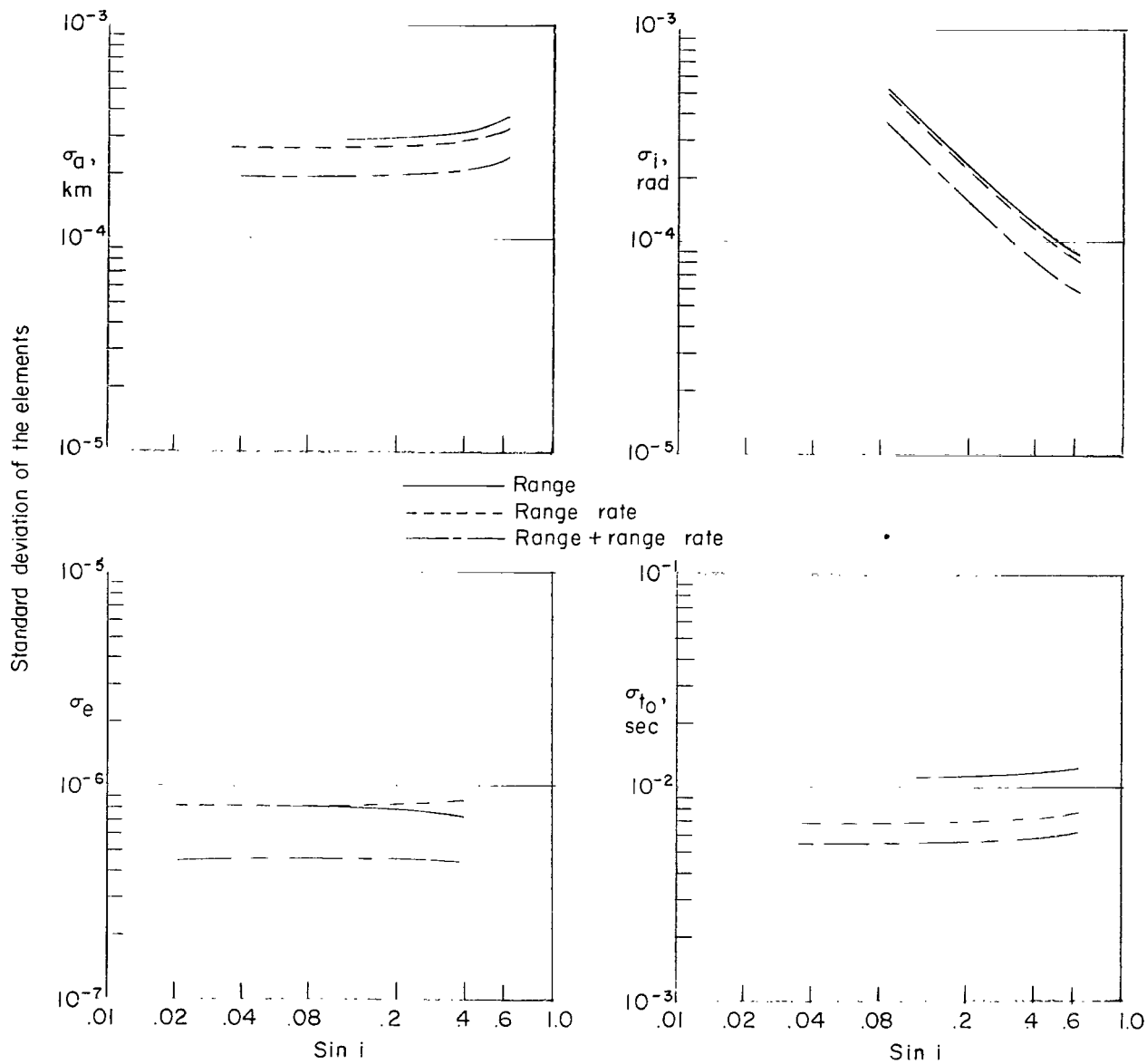


Figure 9.- Variation of the standard deviation of the nominal-orbit elements with the sine of the inclination.

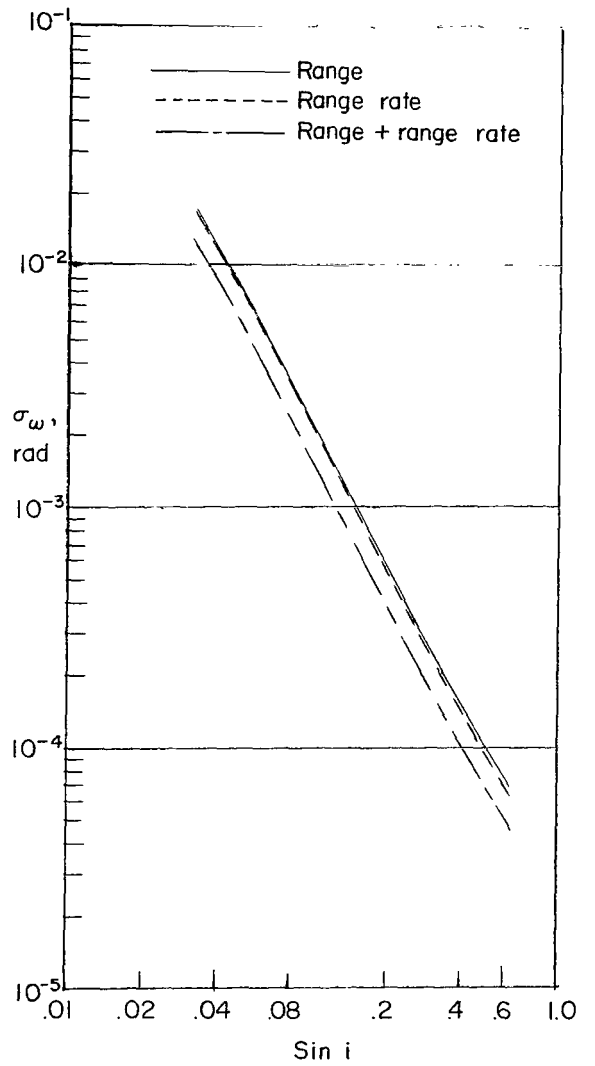
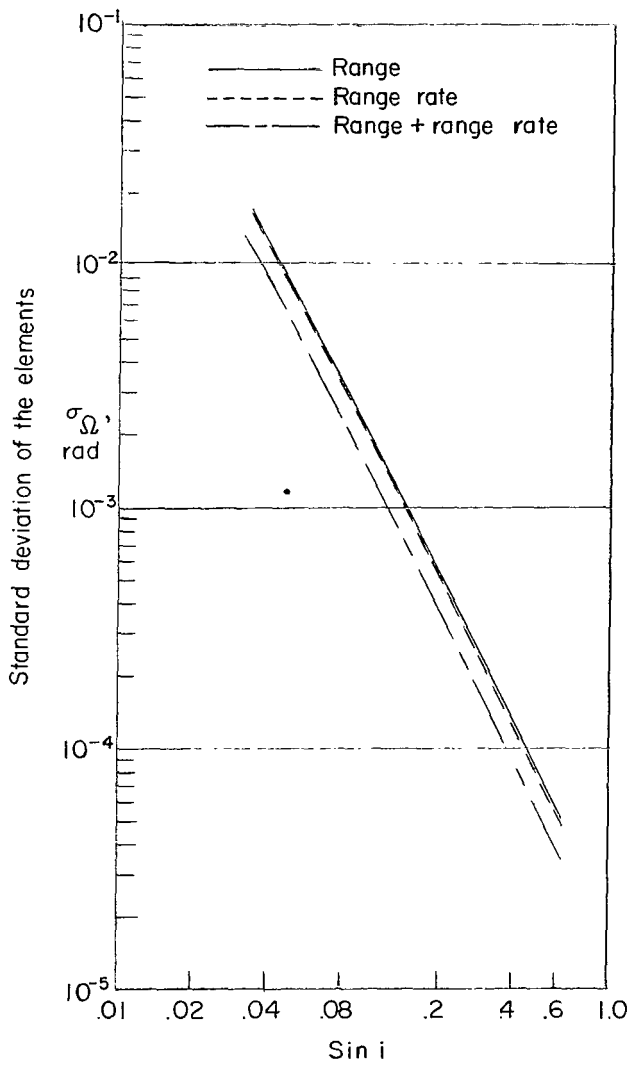


Figure 9.- Concluded.

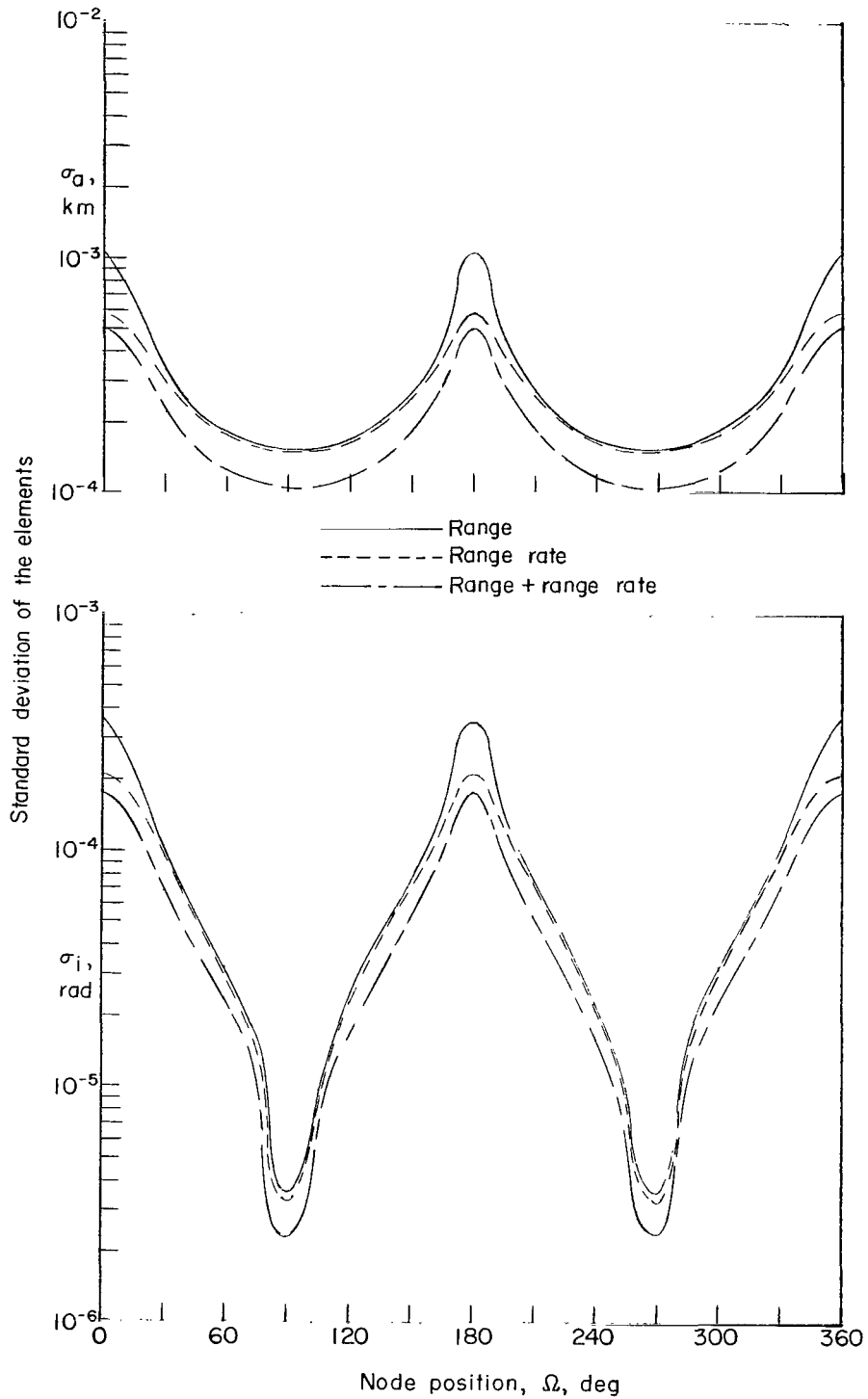


Figure 10.- Variation of the standard deviation of the nominal-orbit elements with the position of ascending node.

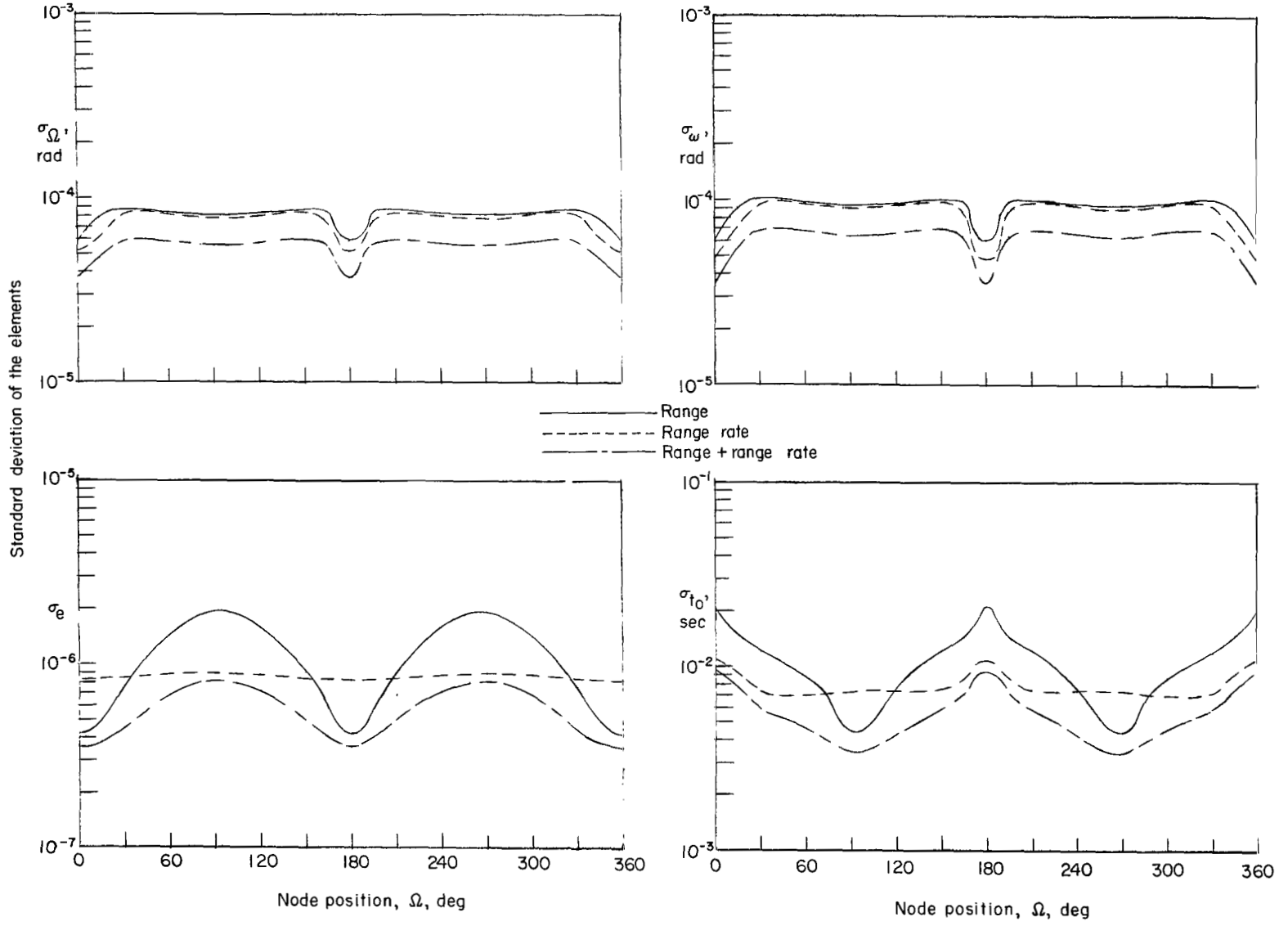


Figure 10.- Concluded.

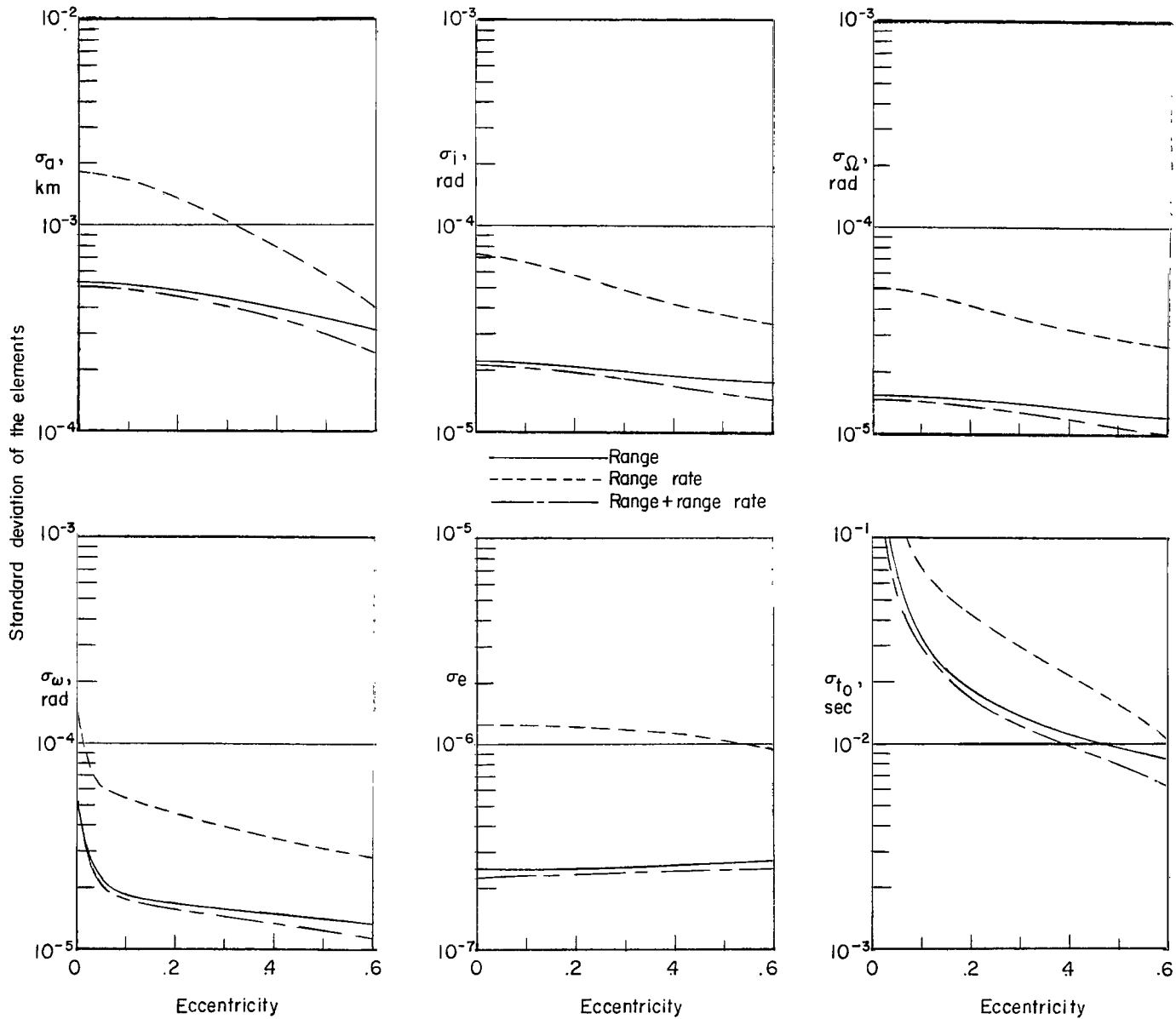


Figure 11.- Variation of the standard deviation of the nominal-orbit elements with eccentricity. (Note that a was fixed at 5000 km.)

3/20/77
E

"The aeronautical and space activities of the United States shall be conducted so as to contribute . . . to the expansion of human knowledge of phenomena in the atmosphere and space. The Administration shall provide for the widest practicable and appropriate dissemination of information concerning its activities and the results thereof."

—NATIONAL AERONAUTICS AND SPACE ACT OF 1958

NASA SCIENTIFIC AND TECHNICAL PUBLICATIONS

TECHNICAL REPORTS: Scientific and technical information considered important, complete, and a lasting contribution to existing knowledge.

TECHNICAL NOTES: Information less broad in scope but nevertheless of importance as a contribution to existing knowledge.

TECHNICAL MEMORANDUMS: Information receiving limited distribution because of preliminary data, security classification, or other reasons.

CONTRACTOR REPORTS: Technical information generated in connection with a NASA contract or grant and released under NASA auspices.

TECHNICAL TRANSLATIONS: Information published in a foreign language considered to merit NASA distribution in English.

TECHNICAL REPRINTS: Information derived from NASA activities and initially published in the form of journal articles.

SPECIAL PUBLICATIONS: Information derived from or of value to NASA activities but not necessarily reporting the results of individual NASA-programmed scientific efforts. Publications include conference proceedings, monographs, data compilations, handbooks, sourcebooks, and special bibliographies.

Details on the availability of these publications may be obtained from:

SCIENTIFIC AND TECHNICAL INFORMATION DIVISION
NATIONAL AERONAUTICS AND SPACE ADMINISTRATION
Washington, D.C. 20546